Harmonic Beamforming in Time-Modulated Linear Arrays

Lorenzo Poli, *Graduate Student Member, IEEE*, Paolo Rocca, *Member, IEEE*, Giacomo Oliveri, *Member, IEEE*, and Andrea Massa, *Member, IEEE*

***Abstract*—In this paper, the synthesis of simultaneous multibeams through time-modulated linear arrays is studied. Unlike classical phased arrays where the antenna aperture is usually shared to generate multiple beams, the periodic on-off sequences controlling the static excitations are properly defined by means of an optimization strategy based on the Particle Swarm algorithm to afford desired multiple patterns at harmonic frequencies to make practical application of these harmonic beams which are typically regarded as an undesirable effect in time-modulated arrays. The synthesis of simultaneous broadside sum and difference patterns, flat-top and narrow beam patterns, and steered multibeams is enabled as assessed by a set of selected results reported and discussed to show the potentialities of the proposed method. Comparisons with previously published results are reported, as well.**

***Index Terms*—Harmonic beams, particle swarm optimization, time-modulated linear arrays.**

I. Introduction

MULTIBEAM antennas are radiating systems devoted to generate multiple patterns from the same aperture. Originally, they were used for surveillance and tracking in radar systems [1], but multiple beam antennas are recently also playing a key role in communication systems installed on satellites and ground stations [2]. As for radars, widebeam patterns are required for search and detection functions, while narrow beams with high angular resolution capabilities are needed for tracking purposes. On the other hand, the advantages of using multiple beams for communication purposes lie in the possibility to manage more communications/services from different spatial directions and to operate over multiple frequency bands. Moreover, patterns with different shapes can be used in adaptive systems to maintain reliable wireless links in the presence of jammers or interference signals or to properly address different requests of service.

Two different solutions have been principally considered in designing multibeam antennas. The former considers reflector antennas, either parabolic structures or reflectarrays, where the primary source is composed by multiple feeds whose output signals can be shared between adjacent patterns to reduce the costs and the complexity of the feeding structure [1]. The other exploits antenna arrays and, nowadays, is the preferred solution since it allows a direct control of the illumination on the aperture and an electronic beam steering. Moreover, array architectures generally have a lighter weight and they can be made conformal.

Dealing with arrays, many strategies have been proposed to synthesize switchable [3] and reconfigurable arrays [4]–[6]. The excitations of switchable arrays are selected among a list of predetermined configurations, whereas the excitations are adaptively controlled (usually only the phase weights to simplify the hardware implementation) in reconfigurable arrays. Since the whole set of array elements is optimized to generate each pattern, high radiation performances can be yielded even though only one beam can be generated at each time instant. To avoid this drawback, other solutions have been proposed to simultaneously radiate multiple patterns. Sub-arrayed antennas as well as interleaved arrays have proved to work properly in both radar [7]–[10] and biomedical [11], [12] applications.

Another approach for the simultaneous generation of multiple-patterns is based on time-modulation (TM). Although its theoretical formulation [13] and the first practical implementations to obtain average ultra-low sidelobe patterns [14] date back to the 1960s, there is nowadays a renewed and growing interest towards such a solution as confirmed by the number of contributions in the reference literature on antennas as well as the applications where timed arrays have been successfully applied. The main limitation of these systems is related to the presence of the sideband radiation (SR) due to the periodic on-off commutations of the RF switches of the beam forming network. However, optimization strategies based on evolutionary algorithms (e.g., differential evolution [15], simulated annealing [16], genetic algorithms [17], and particle swarm optimizer [18]) have recently provided efficient switching schemes to properly address such an issue. It is also worth noting that the theory of TM arrays has been recently revised and formalized in a rigorous mathematical fashion [19], [20], [21] in order to derive analytical relationships for exactly quantifying the power dispersions associated to the SR. For completeness, let us consider that further studies have dealt with the evaluation of the directivity and gain [22] and their optimization [23]. As for the applications, time-modulated arrays have been employed to generate ultra-low sidelobe patterns for the suppression of interferences and clutters [14] and shaped beams [24] with reduced dynamic range ratios. The synthesis of pulse doppler radars [25] and compromise patterns for monopulse radars [26] has been also analyzed, but experimental prototypes have been implemented [17], [27] in a

Manuscript received January 31, 2010; revised October 29, 2010; accepted November 26, 2010. Date of publication May 10, 2011; date of current version July 07, 2011. This work supported in part by the Italian National Project: Wireless multiplatform MIMO Active access networks for QoS-demanding multimedia delivery (WORLD), under Grant 2007R989S.

The authors are with the Department of Information Engineering and Computer Science, University of Trento, Povo 38050 Trento, Italy (e-mail: lorenzo.poli@disi.unitn.it; paolo.rocca@disi.unitn.it; giacomo.oliveri@disi.unitn.it; andrea.massa@ing.unitn.it).

Color versions of one or more of the figures in this paper are available online at http://ieeexplore.ieee.org.

Digital Object Identifier 10.1109/TAP.2011.2152323

few cases and further researches are expected in such a framework. In these works, the harmonic beams are power losses to be minimized, while other approaches consider a different point of view by exploiting the generation of simultaneous patterns at different sidebands. More specifically, patterns with the same shape generated at different harmonics and pointing at different angular directions have been used in radar systems to enable the electronic beam scanning by means of a progressive on-off switching of the array elements [28]. The same concept has been recently revisited in [29] and extended to the estimation of the directions of arrival [30]. Accurate radar localization and tracking capabilities have been assessed in [31] by synthesizing a two-element TM array providing a monopulse-like behavior where two beams (one with a peak and another with a null along the broadside direction) have been generated at the central and first harmonic, respectively.

In this paper, an optimization-based technique for the synthesis of TM linear arrays able to generate multiple beams at different sidebands with different shapes and features is presented. Such a strategy can be used for multi-function radars devoted to surveillance and security purposes [28], [31] as well as for selectively receiving different signals at different sidebands. Moreover, the diversity of different beam patterns with various shapes can be of interest in mobile communications for designing innovative base stations as well as in multiple-input multiple-output (MIMO) systems. The harmonic beamforming is obtained by determining the periodic on-off time sequence that modulates the static excitations of the array by considering an iterative optimization evolving according to the particle swarm (PS) strategy [32]. For a numerical assessment of the proposed approach, simultaneous broadside sum and difference patterns, flat-top and narrow beams, as well as steered multibeams are synthesized.

The paper is organized as follows. The problem is mathematically formulated in Section II where the synthesis procedure is described, as well. Selected results from a set of numerical experiments are presented (Section III) to point out the potentialities of the proposed multibeam strategy. Eventually, some conclusions are drawn (Section IV).

II. Mathematical Formulation

Let us consider a time-modulated linear antenna array (TMLA) where a set of N radio-frequency switches is used to modulate the static excitations of amplitudes A_n, $n = 0, \ldots, N-1$, and phases φ_n, $n = 0, \ldots, N-1$. Such a linear arrangement of N isotropic sources displaced along the z axis at the positions z_n, $n = 0, \ldots, N-1$, radiates the following field [19]

$$F(\theta, t) = e^{j\omega_0 t} \sum_{n=0}^{N-1} A_n e^{j\varphi_n} U_n(t) e^{j\beta z_n \cos\theta} \tag{1}$$

where ω_o is the central angular frequency, $\beta = \omega_0/c$ is the free-space wavenumber, c being the speed of light in vacuum, and θ denotes the angular direction. The RF switches are controlled by means of N digital signals, $U_n(t), n = 0, \ldots, N-1$, of period T_p mathematically modeled as rectangular pulse functions with values $U_n(t) = 1$ within the normalized (with respect to T_p) duration $\tau_n = i_n^f - i_n^r$, $i_n^r, i_n^f \in [0,1]$ being the switch-on (raise) and switch-off (fall) time instants, respectively, and $U_n(t) = 0$ for the remaining part of the modulation period. Because of the time periodicity, each pulse function can be expanded into a Fourier series, $U_n(t) = \sum_{h=-\infty}^{\infty} u_{hn} e^{jh\omega_p t}$, where $\omega_p = 2\pi/T_p$ and the expansion coefficients are equal to $u_{hn} = (1/T_p) \int_{T_p/2}^{-T_p/2} U_n(t) e^{-jh\omega_p t} dt$. Accordingly, (1) can be rewritten as an (ideally) infinite number of radiated patterns shifted of $h\omega_p$ from ω_0

$$F(\theta, t) = \sum_{h \in \mathbb{Z}} F^{(h)}(\theta, t) \tag{2}$$

whose hth term is given by $F^{(h)}(\theta, t) = e^{j(\omega_0 + h\omega_p)t} \sum_{n=0}^{N-1} I_{hn} e^{j\beta z_n \cos\theta}$, $I_{hn} = A_n u_{hn} e^{j\varphi_n}$ $(n = 0, \ldots, N-1)$ being the equivalent excitation. In particular, the pattern at the central frequency is given by $F^{(0)}(\theta, t) = e^{j\omega_0 t} \sum_{n=0}^{N-1} I_{0n} e^{j\beta z_n \cos\theta}$ and the corresponding Fourier coefficients are real and equal to $u_{0n} = \tau_n$, $n = 0, \ldots, N-1$. Otherwise, those at the harmonic frequencies $(h \neq 0)$ are complex and given by [23] (3), shown at the bottom of the page.

It follows that to synthesize desired patterns at the central frequency $(h = 0)$ and at its harmonics $(h \neq 0)$ the set of the pulse durations, $\underline{\tau} = \{\tau_n; n = 0, \ldots, N-1\}$, and the values of the switch-on instants, $\underline{i} = \{i_n^r; n = 0, \ldots, N-1\}$, can be properly optimized. Whether necessary, the sets of amplitudes, $\underline{A} = \{A_n; n = 0, \ldots, N-1\}$, and phases, $\underline{\varphi} = \{\varphi_n; n = 0, \ldots, N-1\}$, of the static excitations can be also properly tuned.

However, it is worthwhile to point out that without suitable countermeasures the power associated to the SR decreases as the harmonic index h increases [19] and only the first harmonic modes $(1 \leq |h| \leq H)$ are expected to generate "useful" patterns. In order to overcome this drawback in view of multiple harmonic beams, the following PS-based optimization procedure is proposed:

- ***Definition of the Static Excitations—$\underline{A}$ and $\underline{\varphi}$***
  The values of the static excitations are generally *a-priori* defined according to the following motivations depending on the problem at hand. The use of unitary amplitude weights (i.e., $A_n = 1$, $n = 0, \ldots, N-1$) is generally preferred in order to simplify the complexity of the beam

$$u_{hn} = \begin{cases} \tau_n sinc(\pi h \tau_n) e^{-j\pi h(\tau_n + 2i_n^r)} & if\ 0 \leq i_n^r \leq (1 - \tau_n) \\ \frac{sin[\pi h(1-i_n^r)] e^{-j\pi h(1+i_n^r)} + sin[\pi h(i_n^r + \tau_n - 1)] e^{-j\pi h(i_n^r + \tau_n - 1)}}{\pi q} & if\ (1 - \tau_n) < i_n^r \leq 1. \end{cases} \tag{3}$$

forming network [16], [17] and to avoid additional amplifiers/attenuators as shown in synthesizing ultra-low sidelobe patterns [14], [33] with a reduced dynamic range. Differently, non-uniform (complex) weights can be used to generate a desired quiescent (without time-modulating the element excitations) pattern at the central frequency ($h = 0$). From an algorithmic point of view, a smaller number of control variables reduces the computational burden required by the optimization process. Otherwise, a better matching of the synthesized solutions with the user-defined requirements can be achieved when more degrees-of-freedom are available;

- ***Definition of the TM Pulse Sequence—$\underline{\tau}$ and $\underline{i}$***
  The parameters modeling the rectangular digital signals, namely the pulse durations, $\underline{\tau}$, and the switch-on instants, $\underline{i}$, are determined by minimizing the cost function, Ψ, aimed at enforcing the desired patterns both at the central frequency, $\omega_0(h = 0)$, and at the first H sideband (upper and lower) radiations, $\omega_0 \pm h\omega_p$, $h = 1, \ldots, H$

$$\Psi(\underline{x}^k) = \sum_{h=-H}^{H} \sum_{\psi=\{SLL,\Theta,|SBL|,RPL\}} w_{\psi}^{(h)} \times \left\{ \Upsilon\left[\psi^{(h)}(\underline{x}^k,\theta) - \psi_{trg}^{(h)}\right] \frac{\left|\psi_{trg}^{(h)} - \psi^{(h)}(\underline{x}^k,\theta)\right|^2}{\left|\psi_{trg}^{(h)}\right|^2} \right\} \quad (4)$$

where $\underline{x} = \{x_u; u = 1, \ldots, U = 2 \times N\}$ is the set of unknown quantities (i.e., $\underline{x} = \underline{\tau} \cup \underline{i}$) and Υ is the Heaviside function. Moreover, $\psi_{trg}^{(h)}$ denotes the target/desired value along the θ direction of the sidelobe level ($\psi \Leftarrow SLL$), the first null beamwidth ($\psi \Leftarrow \Theta$), the sideband level ($\psi \Leftarrow |SBL|$), and the ripple level ($\psi \Leftarrow RPL$) of the hth harmonic pattern. The same notation holds true for the current value $\psi^{(h)}(\underline{x}^k, \theta)$. Furthermore, $w_{\psi}^{(h)}$ is a real and positive coefficient weighting each term of the cost function according to the problem requirements.

In order to minimize (4), a standard PS optimization algorithm [32] is used by iteratively (k being the iteration index, $k = 1, \ldots, K$) applying the following updating equations

$$\begin{aligned} x_{u,s}^k &= x_{u,s}^{k-1} + v_{u,s}^k \\ v_{u,s}^k &= w v_{u,s}^{k-1} + C_1 r_1 \left(p_{u,s}^k - x_{u,s}^k\right) \\ &\quad + C_2 r_2 \left(g_u^k - x_{u,s}^k\right) \end{aligned} \quad (5)$$

where w is the inertial weight coefficient and C_1 and C_2 are the cognitive and social acceleration coefficients, respectively. Moreover, r_1 and r_2 are uniformly-distributed random variables. As far as the swarm is concerned, s ($s = 1, \ldots, S$) is the index of the sth particle, $\underline{p}_s^k = \arg\{\min_{k=1,\ldots,K}[\Psi(\underline{x}_s^k)]\}$ is the personal best particle, while $\underline{g}^k = \arg\{\min_{s=1,\ldots,S;k=1,\ldots,K}[\Psi(\underline{x}_s^k)]\}$ is the global best of the whole swarm at the kth iteration.

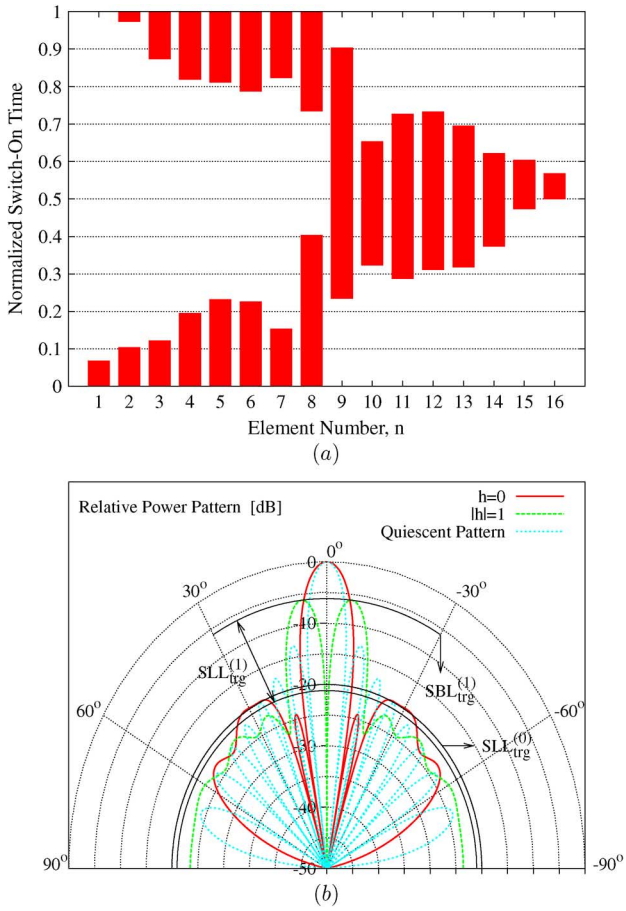

Fig. 1. $\Sigma - \Delta$ *configuration* ($N = 16$, $d = \lambda/2$)—optimized (a) pulse sequence and (b) relative power patterns at the central frequency ($h = 0$—sum pattern) and at the fundamental frequency ($|h| = 1$—difference pattern).

III. Numerical Results

The first experiment deals with the generation of a sum pattern at the central frequency and a difference pattern at the fundamental one ($h = H = 1$) useful in monopulse radars for search-and-track purposes. A linear array with $N = 16$ equally-spaced elements located at $z_n = d \times n$, $n = 0, \ldots, N-1$, $d = \lambda/2$ being the inter-element distance, is the reference architecture. Amplitude-only static excitations with unitary gains have been chosen (i.e., $A_n = 1$ and $\varphi_n = 0, n = 0, \ldots, N-1$) to yield a simple beamforming network. According to the guidelines in [31], here applied to the synthesis of arrays with more than two elements [34], it is enough to energize the two halves of the array with a shift of $T_p/2$ in the time pulse sequence to obtain a pattern with a null on boresight. Therefore, the pulse durations have been set to $\tau_n = \tau_{n+N/2} + 0.5$, $n = 0, \ldots, (N/2) - 1$, and only half elements of the TM array have been optimized by minimizing (4) with $\psi = \{SLL, |SBL|\}$ and $w_{\psi}^{(h)} = 1, h = 0$, 1, the reference values being fixed to $SLL_{trg}^{(0)} = -20$ dB, $SLL_{trg}^{(1)} = -15$ dB, and $SBL_{trg}^{(1)} = -6$ dB. Moreover, the initial configuration of the unknowns has been set to afford a Dolph-Chebyshev pattern with $SLL = -20$ dB at $h = 0$.

Fig. 1(a) shows the configuration of the switch-on times obtained after $K = 2000$ iterations of the PS procedure carried

TABLE I
Sum-Difference Configurations ($N = 16, d = \lambda/2$)—PATTERN INDEXES

	$\Sigma - \Delta$		$\Delta - \Sigma$
	PSO	[34]	*PSO*
$SLL^{(0)}$ $[dB]$	-19.8	-30.0	-16.9
$\Theta_{fn}^{(0)}$ $[deg]$	21.6	21.4	18.4
$SBL^{(1)}$ $[dB]$	-6.0	-6.1	-0.7
$SLL^{(1)}$ $[dB]$	-16.5	-14.6	-16.9
$\Theta_{fn}^{(1)}$ $[deg]$	18.3	28.8	17.8
$P^{(0)}$ %	42.9	37.9	42.4
$P^{(1)}$ %	18.7	20.6	20.7
$SLL_{trg}^{(0)}$ $[dB]$	-20.0		-15.0
$SBL_{trg}^{(1)}$ $[dB]$	-6.0		-1.0
$SLL_{trg}^{(1)}$ $[dB]$	-15.0		-15.0

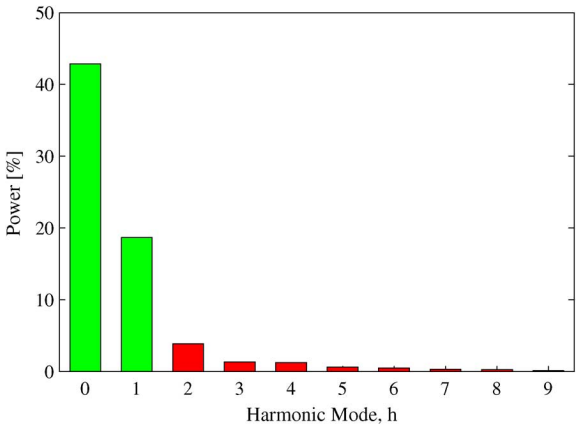

Fig. 2. $\Sigma - \Delta$ *configuration* ($N = 16, d = \lambda/2$)—percentage of the individual power associated to the harmonic radiations.

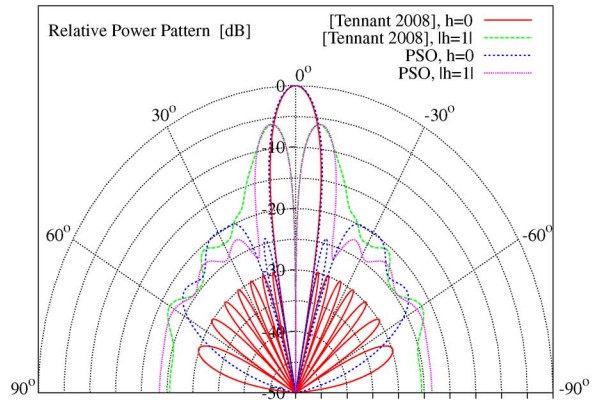

Fig. 3. $\Sigma - \Delta$ *configuration* ($N = 16, d = \lambda/2$)—relative power patterns at the central frequency ($h = 0$—sum pattern) and at the fundamental frequency ($|h| = 1$—difference pattern) synthesized with the PS optimization and in [34].

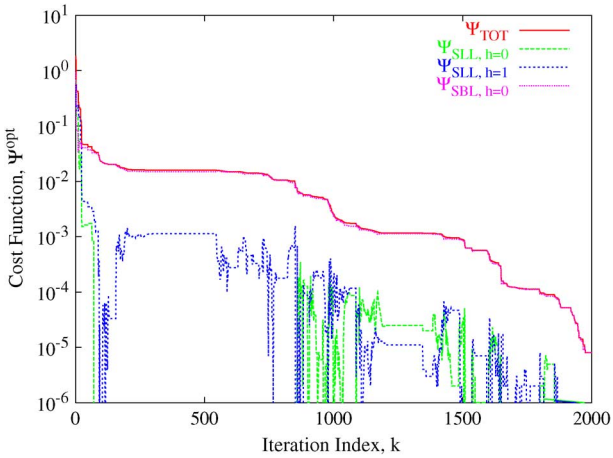

Fig. 4. $\Sigma - \Delta$ *configuration* ($N = 16, d = \lambda/2$)—behavior of the cost function throughout the optimization process and its the individual terms.

out with a swarm of $S = 20$ particles and the control parameters set to a standard configuration [23]: $C_1 = C_2 = 2$ and $w = 0.4$. The radiated patterns are given in Fig. 1(b) for $h = 0$ and $|h| = 1$, while the corresponding pattern indexes are reported in Table I ($\Sigma - \Delta$ configuration). As expected, most of the power is radiated at the central frequency and at the fundamental one with a percentage equal to $P^{(0)} = 42.9\%$ and $P^{(1)} = 18.7\%$ of the total power ($P^{(h)}$ being the power associated to the pattern at the hth harmonic radiation), respectively. Such an outcome is further pointed out in Fig. 2 where the power content of each pattern up to the 9th harmonic mode is reported. The amount of power rapidly tends to zero when the harmonic index h grows. For completeness, the solution with the proposed approach and that in [34] are compared in Fig. 3 to also point out that an unavoidable trade-off exists. As a matter of fact, if a more accurate control of the sidelobes for $|h| = 1$ can be obtained through the PS optimizer, on the other hand, the SLL at $h = 0$ increases with respect to that in [34].

As for the minimization process, Fig. 4 gives an indication of the optimization process by showing the plot of the cost function throughout the iterations.

The second experiment still considers the synthesis of sum and difference patterns, even though now the sum beam is synthesized at $h = 1$, while the difference one at the central frequency ($h = 0$). Towards this end, the odd symmetry of the excitations is enforced to generate a difference beam by adding π to the phase values of half array (i.e., $\varphi = \pi$, $n = 0, \ldots, (N/2) - 1$). The value $SBL_{trg}^{(1)}$ has been set to -1 dB since only one main beam is required at $|h| = 1$. Moreover, the thresholds $SLL_{trg}^{(0)} = SLL_{trg}^{(1)} = -15$ dB have been chosen and all terms of the cost function have been equally weighted.

The optimized switch-on times and the corresponding sum ($|h| = 1$) and difference ($h = 0$) patterns are shown in Fig. 5(a) and (b), respectively. From the quantitative pattern indexes in Table I ($\Delta - \Sigma$ configuration), it turns out that both patterns are quite similar in terms of sidelobe levels (i.e., $SLL^{(0)} = SLL^{(1)} = -16.9$ dB) and sideband values ($SBL^{(1)} = -0.7$ dB). Moreover, $P^{(0)} = 42.4\%$ and $P^{(1)} = 20.7\%$ (Fig. 6). Concerning the sideband radiation, the values of the SBLs of the first 30 harmonic modes of the $\Delta - \Sigma$ solution are reported in Fig. 7(a) and compared with those of the $\Sigma - \Delta$ configuration, as well. Whether for $|h| > 2$ the SBLs have similar behaviors, the advantages of the $\Delta - \Sigma$ solution are non-negligible at the fundamental frequency (i.e., $SBL_{\Delta-\Sigma}^{(1)} = -0.7$ dB vs. $SBL_{\Sigma-\Delta}^{(1)} = -6.0$ dB—Table I).

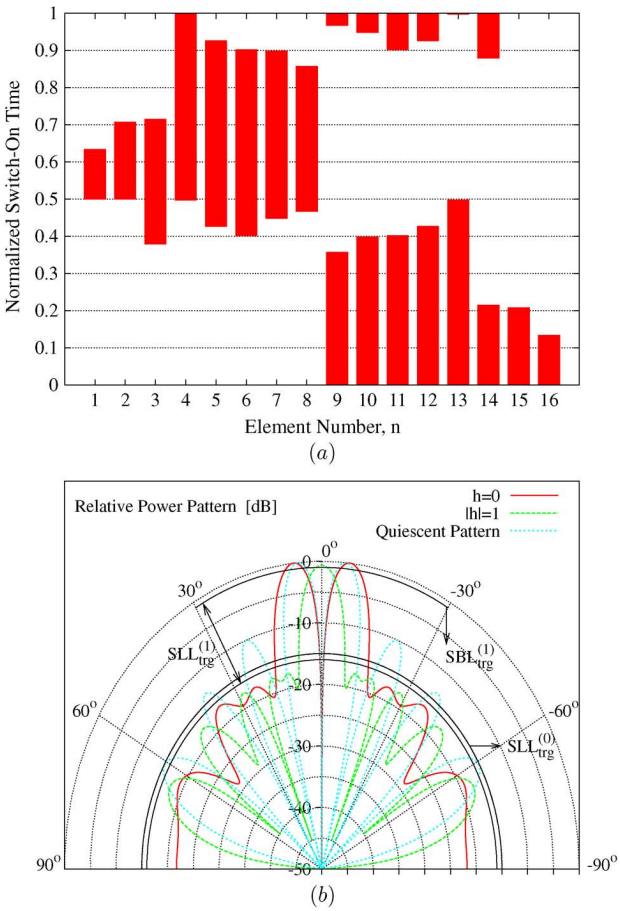

Fig. 5. $\Delta - \Sigma$ *configuration* ($N = 16$, $d = \lambda/2$)—optimized (a) pulse sequence and (b) relative power patterns at the central frequency ($h = 0$—difference pattern) and at the fundamental frequency ($|h| = 1$—sum pattern).

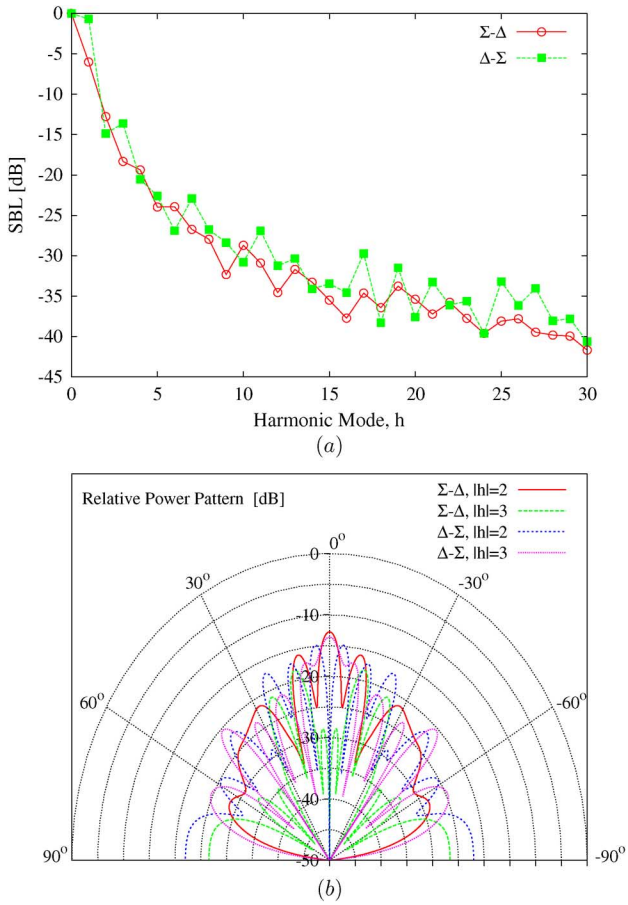

Fig. 7. *Sum-difference configurations* ($N = 16$, $d = \lambda/2$)—comparison of (a) the behavior of the sideband levels $SBL^{(h)}$ when $h \in [1, 30]$ and (b) the harmonic patterns radiated at $|h| = 2, 3$.

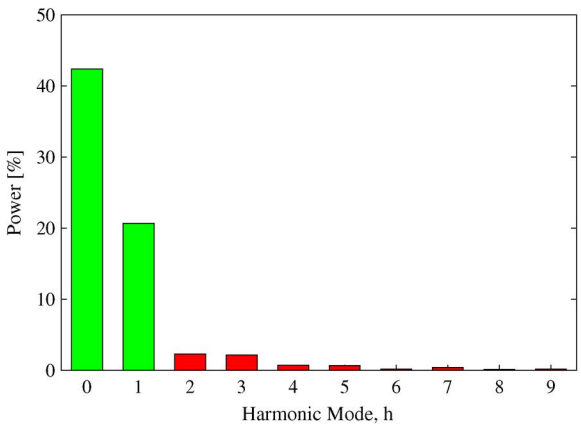

Fig. 6. $\Delta - \Sigma$ *configuration* ($N = 16, d = \lambda/2$)—relative power patterns of the sideband radiation for $|h| = 1, 2, 3$.

For completeness, the radiation patterns at $|h| = 2, 3$ are displayed in Fig. 7(b).

The following experiments are concerned with two design solutions suitable for intercepting signals impinging on an array of $N = 16$ elements spaced by $d = \lambda/2$ from different angular directions without phase shifters in the array architecture. In the first example, the approach exploits the guidelines in [28], recently also considered in [29], where the beam steering at the first harmonic mode is forced by controlling the pulse sequence. Likewise [29], the pattern is requested to be directed at broadside at ω_0, while $\theta_0^{(1)} = -30°$ and $\theta_0^{(-1)} = 30°$ are the directions of the desired beams at the first upper $(h = 1)$ and lower $(h = -1)$ sideband, respectively. Towards this purpose, the cost function has been defined by setting $SBL_{trg}^{(1)}(\theta_0) = SBL_{trg}^{(-1)}(\theta_0) = -2$ dB. Moreover, the reference level of the secondary lobes at $h = 0$ and $h = \pm 1$ has been fixed to -20 dB.

The PS-optimized solution is summarized in Fig. 8 where the on-off sequence [Fig. 8(a)] and the corresponding radiated patterns are shown [Fig. 8(b)]. The indexes in Table II (*Harmonic Beam Steering*) confirm the effectiveness of the proposed strategy in yielding a satisfactory solution that fits the user requirements. The possibility to selectively and simultaneously receive signals from three different directions is the main advantage of such a solution, even though an *ad-hoc* receiver able to separate each harmonic component [29] would be necessary. An alternative solution is presented in Fig. 9 where only one pattern, characterized by two main beams pointing at $\theta_{0,1}^{(1)} = -\theta_{0,2}^{(1)} = -30°$, is generated at the first sideband either at $h = 1$ and not at $h = -1$ or vice versa. Although it is not possible to distinguish whether the signals impinge from $\theta_{0,1}^{(1)}$ or $\theta_{0,2}^{(1)}$, the

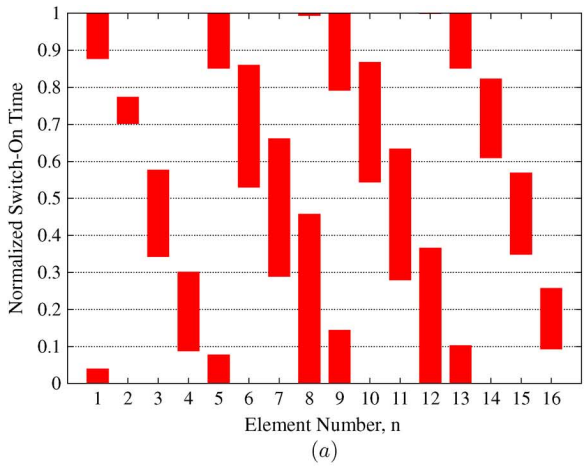

(*a*)

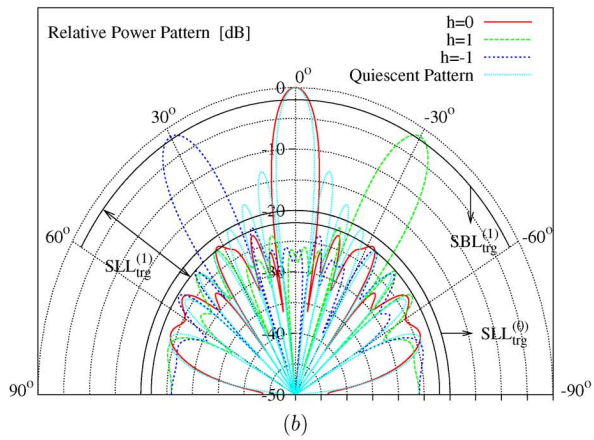

(*b*)

Fig. 8. *Harmonic beam steering* ($N = 16$, $d = \lambda/2$)—optimized (*a*) pulse sequence and (*b*) relative power patterns at the central frequency [$h = 0$—broadside beam ($\theta_0^{(0)} = 0°$)] and at the fundamental frequencies [$h = 1$—steered beam ($\theta_0^{(1)} = -30°$); $h = -1$—steered beam ($\theta_0^{(-1)} = 30°$)].

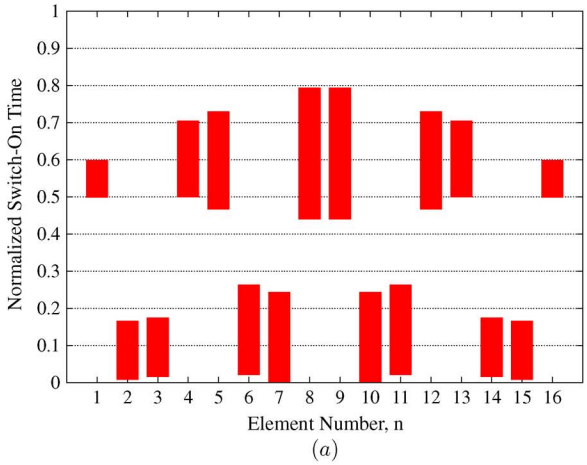

(*a*)

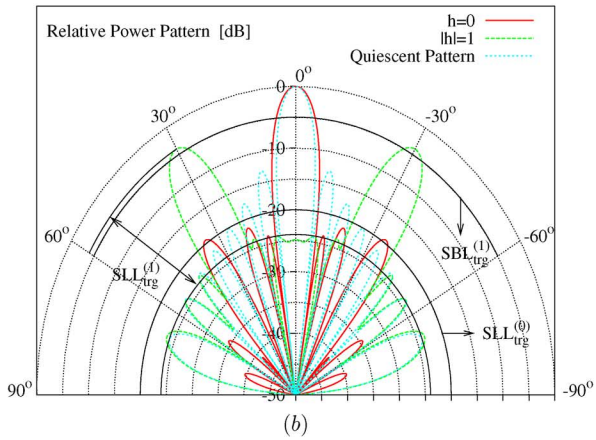

(*b*)

Fig. 9. *Double sum configuration* ($N = 16$, $d = \lambda/2$)—optimized (*a*) pulse sequence and (*b*) relative power patterns at the central frequency ($h = 0$—broadside beam ($\theta_0^{(0)} = 0°$)] and at the fundamental frequency [$|h| = 1$—steered beam, $\theta_0^{(h)} = \pm 30°$].

TABLE II
Harmonic Beam Steering—Double Sum Configuration ($N = 16$, $d = \lambda/2$)—PATTERN INDEXES

	Harmonic Beam Steering			*Double Sum Beam*	
	$h = 0$	$h = 1$	$h = -1$	$h = 0$	$\|h\| = 1$
$SLL^{(h)}$ $[dB]$	-21.6	-20.0	-20.0	-19.5	-19.2
Θ_{fn}^{h} $[deg]$	19.6	20.6	20.6	19.0	21.1
$SBL^{(h)}$ $[dB]$	–	-1.5	-1.5	–	-4.0
$\theta_0^{(h)}$ $[deg]$	0	-30.0	30.0	0	± 30
$P^{(h)}$ %	30.5	20.7	20.7	24.0	18.9
$SLL_{trg}^{(h)}$ $[dB]$	-20.0	-20.0	-20.0	-20.0	-20.0
$SBL_{trg}^{(h)}$ $[dB]$	–	-2	-2	–	-5.0

TABLE III
Flat top and Sum Configuration ($N = 12, d = \lambda/2$)—INITIAL ($k = 0$) SETTING [35] FOR THE ITERATIVE OPTIMIZATION

n	φ_n	τ_n
0	0	0.17
1	π	0.03
2	π	0.20
3	π	0.08
4	0	0.46
5	0	1.00
6	0	1.00
7	0	0.46
8	π	0.08
9	π	0.20
10	π	0.03
11	0	0.17

HW implementation is less complex in this case since the received power is collected only at ω_0 and $\omega_1 = \omega_0 + \omega_p$. The indexes describing the synthesized *Double Sum Beam* are summarized in Table II where the performances of the *Harmonic Beam Steering* solution are also reported for comparison.

The last test case is a representative example aimed at showing some other potentialities of the proposed approach. More specifically, the synthesis of a flat-top pattern at ω_0 and of a sum pattern at ω_1 is addressed by considering an array of $N = 12$ half-wavelength spaced elements with uniform amplitude weights (i.e., $A_n = 1$, $n = 0, \ldots, N-1$). The phase weights, $\underline{\varphi}$, and switch-on times, $\underline{i}$, have been initialized ($k = 0$) to afford a flat-top beam as in [35] and their normalized values are reported in Table III. The synthesis targets have been fixed to $SLL_{trg}^{(0)} = SLL_{trg}^{(1)} = -15$ dB and $SBL_{trg}^{(1)} = -2$ dB.

The pulse sequence determined with the PS is shown in Fig. 10(*a*) together with the synthesized two patterns [Fig. 10(*b*)] whose descriptive indexes are reported in

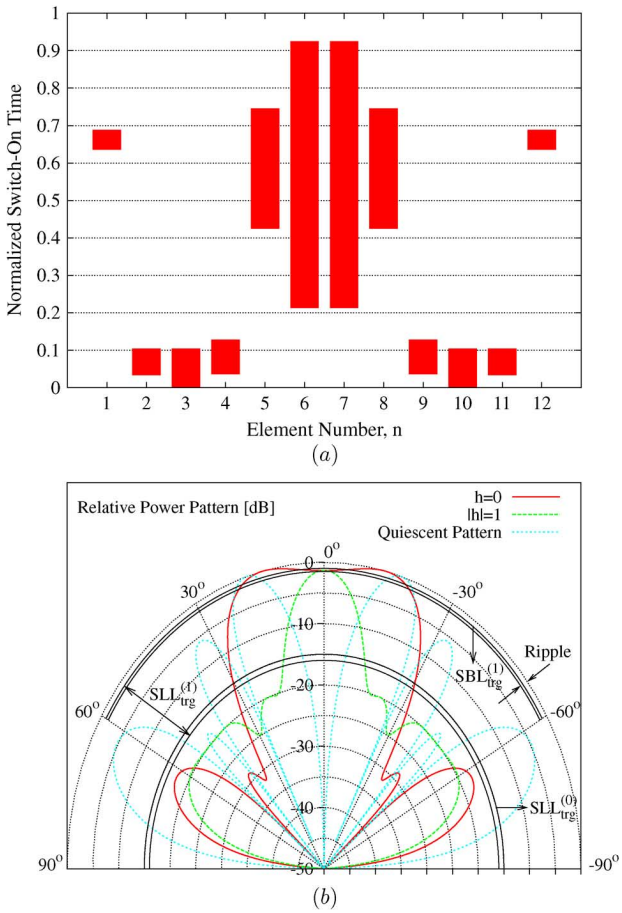

Fig. 10. *Flat top and sum configuration* ($N = 12$, $d = \lambda/2$)—optimized (*a*) pulse sequence and (*b*) relative power patterns at the central frequency ($h = 0$—flat-top pattern) and at the fundamental frequency [$|h| = 1$—sum pattern)].

TABLE IV
Flat top and Sum Configuration ($N = 12$, $d = \lambda/2$)—PATTERN INDEXES

	$Flat-top\ and\ Sum\ Beam$	
	$h=0$	$\lvert h\rvert=1$
$SLL^{(h)}$ $[dB]$	-17.6	-18.5
Γ $[dB]$	1.3	–
$SBL^{(h)}$ $[dB]$	–	-1.3
$P^{(h)}$ %	60.1	8.2
$SLL^{(h)}_{trg}$ $[dB]$	-15.0	-15.0
$SBL^{(h)}_{trg}$ $[dB]$	–	-2
Γ_{trg} $[dB]$	1.5	–

Table IV. As it can be observed, the beams satisfy the design constraints with the level of the secondary lobes equal to $SLL^{(0)} = -17.6$ dB, $SLL^{(1)} = -18.5$ dB, and the peak of the sum beam with value $SBL^{(1)} = -1.3$ dB. Moreover, the flat-top region presents a ripple level (Γ) with a maximum oscillation of $\Gamma = 1.3$ dB ($\Gamma_{trg} = 1.5$ dB).

IV. CONCLUSIONS

In this paper, the synthesis of multiple harmonic beams in time modulated linear arrays has been addressed. The sideband radiations arising from the periodic time-modulation of the static excitations of the array, usually regarded as power losses to avoid, have been profitably exploited to design an antenna system providing simultaneous multiple patterns. Towards this purpose, an optimization procedure has been applied to determine the time-domain descriptors of the digital time sequence that controls the RF switches devoted to implement the time-modulation of the array. Since the power associated to the harmonic modes rapidly reduces for higher harmonic modes, the desired patterns have been synthesized at the central and the first harmonics. Although further investigations are currently under development, the results of the numerical assessment provide a proof that time-modulated arrays are an effective and reliable architectural solution for those applications requiring a multiple and simultaneous beamforming.

ACKNOWLEDGMENT

The authors are grateful to the anonymous reviewers for their technical comments and suggestions.

REFERENCES

[1] I. M. Skolnik, *Radar Handbook*, 3rd ed. New York: McGraw-Hill, 2008.
[2] C. A. Balanis, *Antenna Theory: Analysis and Design*, 3rd ed. Hoboken, NJ: Wiley, 2005.
[3] M. Barba, J. E. Page, J. A. Encinar, and J. R. Montejo-Garai, "A switchable multiple beam antenna for GSM-UMTS base stations in planar technology," *IEEE Trans. Antennas Propag.*, vol. 54, no. 11, pp. 3087–3094, Nov. 2006.
[4] M. Durr, A. Trastoy, and F. Ares, "Multiple-pattern linear antenna arrays with single prefixed amplitude distributions: Modified Woodward-Lawson synthesis," *Electron. Lett.*, vol. 36, no. 16, pp. 1345–1346, Aug. 2000.
[5] A. Trastoy, Y. Rahmat-Samii, F. Ares, and E. Moreno, "Two-pattern linear array antenna: Synthesis and analysis of tolerance," *IEE Proc. Microw. Antennas Propag.*, vol. 151, no. 2, pp. 127–130, Apr. 2004.
[6] M. Comisso and R. Vescovo, "Multi-beam synthesis with null constraints by phase control for antenna arrays of arbitrary geometry," *Electron. Lett.*, vol. 43, no. 7, pp. 374–375, Mar. 2007.
[7] R. L. Haupt, "Interleaved thinned linear arrays," *IEEE Trans. Antennas Propag.*, vol. 53, no. 9, pp. 2858–2864, Sep. 2005.
[8] I. E. Lager, C. Trampuz, M. Simeoni, and L. P. Ligthart, "Interleaved array antennas for FMCW radar applications," *IEEE Trans. Antennas Propag.*, vol. 57, no. 8, pp. 2486–2490, Aug. 2009.
[9] G. Oliveri and A. Massa, "Fully-interleaved linear arrays with predictable sidelobes based on almost difference sets," *IET Radar Sonar Navigat.*, vol. 4, no. 5, pp. 649–661, 2010.
[10] G. Oliveri, P. Rocca, and A. Massa, "Interleaved linear arrays with difference sets," *Electron. Lett.*, vol. 46, no. 5, pp. 323–324, 2010.
[11] A. Austeng and S. Holm, "Sparse 2-D arrays for 3-D phased array imaging—Design methods," *IEEE Trans. Ultrason., Ferroelect., Freq. Contr.*, vol. 49, no. 8, pp. 1073–1086, Aug. 2002.
[12] G. Oliveri and A. Massa, "ADS-based array design for 2D and 3D ultrasound imaging," *IEEE Trans. Ultrason., Ferroelect., Freq. Contr.*, vol. 57, no. 7, pp. 1568–1582, Jul. 2010.
[13] H. E. Shanks and R. W. Bickmore, "Four-dimensional electromagnetic radiators," *Canad. J. Phys.*, vol. 37, pp. 263–275, Mar. 1959.
[14] W. H. Kummer, A. T. Villeneuve, T. S. Fong, and F. G. Terrio, "Ultra-low sidelobes from time-modulated arrays," *IEEE Trans. Antennas Propag.*, vol. 11, no. 6, pp. 633–639, Jun. 1963.
[15] S. Yang, Y. B. Gan, and A. Qing, "Sideband suppression in time-modulated linear arrays by the differential evolution algorithm," *IEEE Antennas Wireless Propag. Lett.*, vol. 1, pp. 173–175, 2002.
[16] J. Fondevila, J. C. Brégains, F. Ares, and E. Moreno, "Optimizing uniformly excited linear arrays through time modulation," *IEEE Antennas Wireless Propag. Lett.*, vol. 3, pp. 298–301, 2004.
[17] S. Yang, Y. B. Gan, A. Qing, and P. K. Tan, "Design of a uniform amplitude time modulated linear array with optimized time sequences," *IEEE Trans. Antennas Propag.*, vol. 53, no. 7, pp. 2337–2339, Jul. 2005.
[18] L. Poli, P. Rocca, L. Manica, and A. Massa, "Handling sideband radiations in time-modulated arrays through particle swarm optimization," *IEEE Trans. Antennas Propag.*, vol. 58, no. 4, pp. 1408–1411, Apr. 2010.

[19] J. C. Brégains, J. Fondevila, G. Franceschetti, and F. Ares, "Signal radiation and power losses of time-modulated arrays," *IEEE Trans. Antennas Propag.*, vol. 56, no. 6, pp. 1799–1804, Jun. 2008.
[20] L. Poli, P. Rocca, L. Manica, and A. Massa, "Pattern synthesis in time-modulated linear arrays through pulse shifting," *IET Microw., Antennas Propag.*, vol. 4, no. 9, pp. 1157–1164, 2010.
[21] L. Poli, P. Rocca, L. Manica, and A. Massa, "Time modulated planar arrays—Analysis and optimization of the sideband radiations," *IET Microw. Antennas Propag.*, vol. 4, no. 9, pp. 1157–1164, 2010.
[22] S. Yang, Y. B. Gan, and P. K. Tan, "Evaluation of directivity and gain for time-modulated linear antenna arrays," *Microw. Opt. Technol. Lett.*, vol. 42, no. 2, pp. 167–171, Jul. 2004.
[23] L. Manica, P. Rocca, L. Poli, and A. Massa, "Almost time-independent performance in time-modulated linear arrays," *IEEE Antennas Wireless Propag. Lett.*, vol. 8, pp. 843–846, 2009.
[24] S. Yang, Y. B. Gan, and P. K. Tan, "A new technique for power-pattern synthesis in time-modulated linear arrays," *IEEE Antennas Wireless Propag. Lett.*, vol. 2, pp. 285–287, 2003.
[25] G. Li, S. Yang, and Z. Nie, "A study on the application of time modulated antenna arrays to airborne pulsed doppler radar," *IEEE Trans. Antennas Propag.*, vol. 57, no. 5, pp. 1579–1583, May 2009.
[26] J. Fondevila, J. C. Brégains, F. Ares, and E. Moreno, "Application of time modulation in the synthesis of sum and difference patterns by using linear arrays," *Microw. Opt. Technol. Lett.*, vol. 48, no. 5, pp. 829–832, May 2006.
[27] A. Tennant and B. Chambers, "Time-switched array analysis of phase-switched screens," *IEEE Trans. Antennas Propag.*, vol. 57, no. 3, pp. 808–812, Mar. 2009.
[28] H. Shanks, "A new technique for electronic scanning," *IRE Trans. Antennas Propag.*, vol. 9, no. 2, pp. 162–166, Mar. 1961.
[29] G. Li, S. Yang, Y. Chen, and Z. Nie, "A novel electronic beam steering technique in time modulated antenna arrays," *Progr. Electromagn. Res.*, vol. 97, pp. 391–405, 2009.
[30] G. Li, S. Yang, and Z. Nie, "Direction of arrival estimation in time modulated antenna arrays with unidirectional phase center motion," *IEEE Trans. Antennas Propag.*, vol. 58, no. 4, pp. 1105–1111, Apr. 2009.
[31] A. Tennant and B. Chambers, "Two-element time-modulated array with direction-finding properties," *IEEE Antennas Wireless Propag. Lett.*, vol. 6, pp. 64–65, 2007.
[32] J. Kennedy, R. C. Eberhart, and Y. Shi, *Swarm Intelligence*. San Francisco, CA: Morgan Kaufmann, 2001.
[33] S. Yang, "Study of low sidelobe time modulated linear antenna arrays at millimeter-waves," *Int. J. Infrared Milli. Waves*, vol. 26, no. 3, pp. 443–456, Mar. 2005.
[34] A. Tennant and B. Chambers, "Control of the harmonic radiation patterns of time-modulated antenna arrays," presented at the IEEE AP-S Int. Symp., San Diego, CA, Jul. 5–12, 2008.
[35] Y. U. Kim and R. S. Elliot, "Shaped-pattern synthesis using pure real distributions," *IEEE Trans. Antennas Propag.*, vol. 36, no. 11, pp. 1645–1649, Nov. 1988.

Lorenzo Poli (S'10) received the M.S. degree in telecommunication engineering from the University of Trento, Italy, in 2008.

He is with the International Graduate School in Information and Communication Technologies, University of Trento and a member of the ELEDIA Research Group. His main interests are the synthesis of the antenna array and electromagnetic inverse scattering.

Paolo Rocca (M'09) received the B.S., M.S., and Ph.D. degrees in telecommunications engineering from the University of Trento, Italy, in 2004, 2005, and 2009, respectively.

He is with the International Graduate School in Information and Communication Technologies, University of Trento and a member of the ELEDIA Research Group. His main interests are in the framework of antenna synthesis and design, electromagnetic inverse scattering, and optimization techniques for electromagnetics.

Giacomo Oliveri (M'09) received the B.S. and M.S. degrees in telecommunications engineering and the Ph.D. degree in space sciences and engineering from the University of Genoa, Italy, in 2003, 2005, and 2009, respectively.

Since 2008, he has been a member of the Electromagnetic Diagnostic Laboratory, University of Trento, Italy. His research work is mainly focused on cognitive radio systems, electromagnetic direct and inverse problems, and antenna array design and synthesis.

Andrea Massa (M'03) received the "Laurea" degree in electronic engineering and Ph.D. degree in electronics and computer science from the University of Genoa, Genoa, Italy, in 1992 and 1996, respectively.

From 1997 to 1999, he was an Assistant Professor of electromagnetic fields at the Department of Biophysical and Electronic Engineering, University of Genoa, teaching the university course of Electromagnetic Fields 1. From 2001 to 2004, he was an Associate Professor and, since 2005, he has been a Full Professor of electromagnetic fields at the University of Trento, where he currently teaches electromagnetic fields, inverse scattering techniques, antennas and wireless communications, and optimization techniques. At present, he is the Director of the ELEDIALab, University of Trento and Deputy Dean of the Faculty of Engineering. His research work since 1992 has been principally on electromagnetic direct and inverse scattering, microwave imaging, optimization techniques, wave propagation in presence of nonlinear media, wireless communications and applications of electromagnetic fields to telecommunications, medicine and biology.

Prof. Massa is a member of the PIERS Technical Committee, the Inter-University Research Center for Interactions Between Electromagnetic Fields and Biological Systems (ICEmB) and Italian representative in the General Assembly of the European Microwave Association (EuMA).